

Numerical and Experimental Investigations of the Effect of Melt Delivery Nozzle Design on the Open- to Closed-Wake Transition in Closed-Coupled Gas Atomization



SHAHED MOTAMAN, ANDREW M. MULLIS, ROBERT F. COCHRANE,
and DUNCAN J. BORMAN

The single-phase gas-flow behavior of a closed-coupled gas atomization was investigated with four different melt nozzle tip designs with two types of gas die. Particular attention was paid to the open- to closed-wake transition. Experimental Schlieren imaging and numerical modeling techniques were employed, with good agreement between the two being found in relation to the wake closure pressure. It was found that the melt nozzle tip design had a significant impact on the WCP, as did the type of die used, with a convergent–divergent gas die giving significantly high WCPs.

DOI: 10.1007/s11663-015-0346-6

© The Minerals, Metals & Materials Society and ASM International 2015

I. INTRODUCTION

THE gas atomization process, particularly Closed-Coupled Gas Atomization (CCGA), is an efficient method for the production of ultrafine, highly spherical metal powders. In principle, CCGA is straightforward: high-pressure gas jets impinging upon a molten metal stream are used to disrupt the stream, breaking it into a spray of fine droplets. The gas is delivered *via* a die that will typically be of either the annular slit or discrete jet type. In an annular slit die, the gas passes through a narrow channel between the die and the outer surface of the melt delivery nozzle, while in a discrete jet die, the gas is delivered through holes machined directly into the die. Liquid metal is then fed down the central bore of the melt delivery nozzle, wherein the former wets the nozzle tip (a process termed pre-filming, which is itself dependent upon the gas-flow conditions) and is stripped off the circumferential edge of the nozzle by the gas (see Figure 1). However, due to hydrodynamic and thermal interaction between the high-pressure gas jets and the molten metal stream, especially near the tip of the melt delivery nozzle, the technique is in practice very complex

and challenging for both academic understanding and industrial practice. The gas-flow pattern around the melt delivery nozzle plays a crucial role in the gas atomization process and may affect the particle size distribution and atomization efficiency.

In previous studies, the gas-flow pattern around the melt delivery nozzle has been divided into two parts: the near-field and the far-field regions. The near-field is an area ranging from 3 to 4 D (D being the diameter of the tip of the melt delivery nozzle at which pre-filming occurs; see Figure 1) downstream of the melt nozzle tip and in which primary breakup occurs. Beyond this is referred to as far-field and is the region in which secondary breakup occurs.

Typical gas-flow patterns for a closed-coupled atomizer are shown in Figure 1. The gas exiting the die is underexpanded, and upon encountering the low pressure region near the melt delivery nozzle, will expand rapidly before compressing again, forming a series of recompression shocks. The reflection of the expansion wave from the sonic boundary will form an internal shock wave at the tip of the melt delivery nozzle. The region of recirculating subsonic gas directly below the melt nozzle and bounded by the sonic boundary and recompression shocks is the wake region, also sometimes referred to as the recirculation zone. It is here that primary breakup occurs.

Various studies, including those by Anderson *et al.*,^[1,2] Ting *et al.*^[3] and Mates *et al.*^[4,5], have observed two possible forms for the wake region depending upon the gas inlet pressure. At high gas pressure, the internal shocks expand downstream in front of the melt delivery nozzle, crossing to form a Mach disk. This gives rise to high pressure at the atomization tip and is termed the closed-wake condition. Conversely, at lower gas inlet pressure a Mach disk will not be present, leading to the open-wake condition, which gives a region of low

SHAHED MOTAMAN, CFD Research Fellow, is with the Institute for Innovation in Sustainable Engineering, University of Derby, Derby, U.K. and also with the Institute of Materials Research, Faculty of Engineering, School of Process, Environmental and Materials Engineering, University of Leeds, Leeds, LS2 9JT, U.K. Contact e-mails: s.motaman@derby.ac.uk; shahed.motaman@gmail.com ANDREW M. MULLIS, Professor, Director, and ROBERT F. COCHRANE, Senior Lecturer, Head of Materials Programs, are with the Institute of Materials Research, Faculty of engineering, School of Process, Environmental and Materials Engineering, University of Leeds. DUNCAN J. BORMAN, Lecturer, is with Engineering Mathematics and Modelling, School of Civil Engineering, University of Leeds, Leeds.

Manuscript submitted July 15, 2014.

Article published online April 17, 2015.

pressure at the melt delivery nozzle tip. They observed that the wake shape in front of the melt nozzle tip affects the atomization process by increasing the over-ambient pressure in the wake region in the closed-wake condition and hence decreasing the melt flow rate inside the melt delivery nozzle. Conversely, the open-wake condition causes sub-ambient pressure in the wake region and increases the melt flow rate inside the melt delivery nozzle. The gas pressure above which the wake region is in the closed condition, and below which it is in the open condition, is termed the wake closure pressure (WCP).

Mates *et al.*,^[4,5] Anderson *et al.*^[6] and Ting *et al.*^[3,7] have reported the WCP to be dependent on a variety of parameters such as: gas die inlet pressure, gas die apex angle, and the external geometry of the melt delivery nozzle. In addition, they observed that different gas die designs, for instance, the use of choked jets or those with

a convergent-divergent (C-D) profile, could affect the gas-flow field at the melt delivery nozzle tip and consequently the WCP. For gas jets in which the internal profile is cylindrical or purely convergent, choked flow will occur, with a maximum exit velocity of Mach 1 and rapid, unconstrained expansion of the gas upon exit. Conversely, for a C-D jet, efficient expansion of the gas inside the jet permits a controlled expansion of the gas with supersonic exit velocity. For a given operating pressure, the mass flow rate is normally determined by the outlet area for a plain jet and by the throat area (the region of minimum cross section where the profile changes from convergent to divergent) for a C-D jet. The mass flow rates can therefore be significantly different between the two geometries unless the pipe/throat diameters have been selected accordingly.

Wake closure is an area of interest in the study of gas atomization because, as reported by Ting *et al.*,^[3] it is believed that operating the system at a pressure just above the WCP is beneficial for producing finer and more uniform powders. A number of researchers have therefore investigated the factors affecting WCP, both experimentally and numerically.

Mi *et al.*^[8] compared the results of numerical simulation of gas-only flow around a melt nozzle with experimental data. The variation of recirculation zone length, WCP, and Mach disk formation with atomization gas pressure were investigated with good agreement being found between the simulations and experimental data. They demonstrated the gas-flow behavior around the melt nozzle is a strong function of atomization gas pressures. Moreover, their numerical results indicated that the open- to closed-wake transition is strongly affected by changing the melt nozzle length. Tong *et al.*^[9] and Xinming *et al.*^[10] reported a comparison of numerical and Schlieren imaging studies on the WCP as a function of atomization gas pressures using an annular

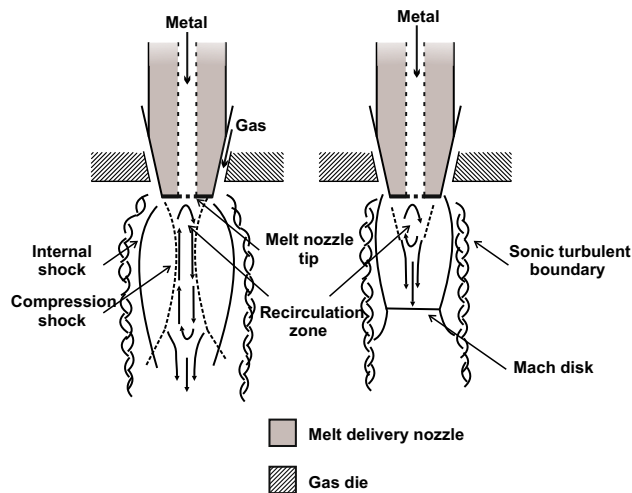


Fig. 1—Schematic diagram of gas-only flow in a CCGA system in the (left) open- and (right) closed-wake conditions.

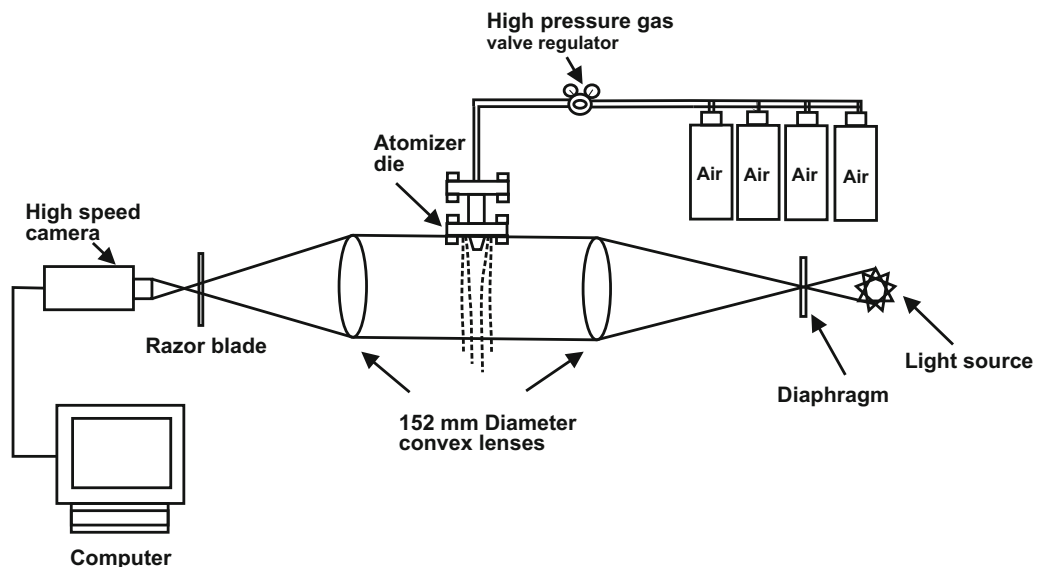


Fig. 2—Schematic view of the Töpler Schlieren apparatus used to image gas flow in the analog atomizer.

slit C–D die. They used a flat-tipped melt delivery nozzle and showed the numerical simulation of the gas-flow field to be in a good agreement with images obtained with the same nozzle and die design in Schlieren imaging experiments, although they found that the experimentally determined WCP was systematically slightly higher than in the numerical simulations.

Ting *et al.*^[7] have presented a Computational Fluid Dynamics (CFD) study of the open to closed-wake transition in the CCGA process. They numerically modeled single-phase gas flow around a flat tipped melt nozzle with a choked gas die as a function of gas pressures. Their numerical results showed two separate zones of primary and secondary recirculation zone in front of the melt delivery nozzle, together with Mach disk formation in the closed-wake condition.

Mates *et al.*^[4,5] have used the Schlieren imaging technique to study single-phase gas flow around a melt delivery nozzle with a flat tipped head and with two die types, one with convergent jets and the other with C–D jets. They observed the open- to closed-wake transition *via* the formation of a Mach disk at a gas pressure of 5.2 MPa for the convergent gas die, but reported the open-wake condition persisted for the C–D gas die to pressure above 5.2 MPa.

Where the effect of melt nozzle geometry has previously been studied on the open- to closed-wake transition, this has been observed as a function of the external nozzle geometry. This paper presents a study in which the Schlieren imaging technique and CFD simulation for single-phase gas flow are used to investigate the open- to closed-wake transition for four different melt nozzles, all of which have same external geometry, but with different internal profiles. Furthermore, both choked and C–D gas dies were used in combination with these melt nozzles and the results compared.

II. EXPERIMENTAL PROCESS

To visualize the gas flow around the melt delivery nozzle, an analog atomizer has been constructed to study the single-phase gas flow as a function of die and nozzle geometry in absence of a second, atomized fluid (*i.e.*, metal). The Töpler Schlieren lens arrangement has been chosen for observing the gas-flow field. Air was used as the atomizing gas and was supplied from four 0.08 m³ cylinders with the maximum pressure of 20 MPa. The cylinders were connected to the inlet side of a high-pressure regulator to supply a steady gas flow to the gas die at pressures up to 5 MPa. A schematic view of the analog atomizer and Töpler Schlieren set-up is shown in Figure 2. The Schlieren images were recorded with a high-speed digital motion analyzer operating at a frame rate of 15,000 fps and a resolution of 750 × 750 pixels. The field of view during these experiments was typically from the nozzle exit to 10 D downstream from the nozzle exit, and the duration of each experiment was about 3.5 seconds. This running time was chosen due to the maximum recording time of the high-speed camera at the selected image resolution. This imaging confirmed that the gas flow was extremely

steady throughout the duration of the experiment, and for this reason, we have used selected stills as being representative of the flow.

The gas die systems for both choked flow and C–D flow comprise a discrete jet arrangement with 18 holes and an apex angle of 45 deg. The C–D die was designed with a throat diameter of 0.4 mm and an exit diameter of 0.68 mm. Standard isentropic flow theory then gives the gas exit velocity as Mach 2.6 with the ratio of inlet/outlet pressure as 19.95, giving an ideal operating pressure of ~2 MPa (assuming the outlet is at standard atmospheric pressure). The 18 C–D jets were machined into the blank die by first drilling a cylindrical pilot hole to the throat diameter. The die was then placed on a specially constructed gimbal, with EDM machining being used to open the outlet of the jet to the desired

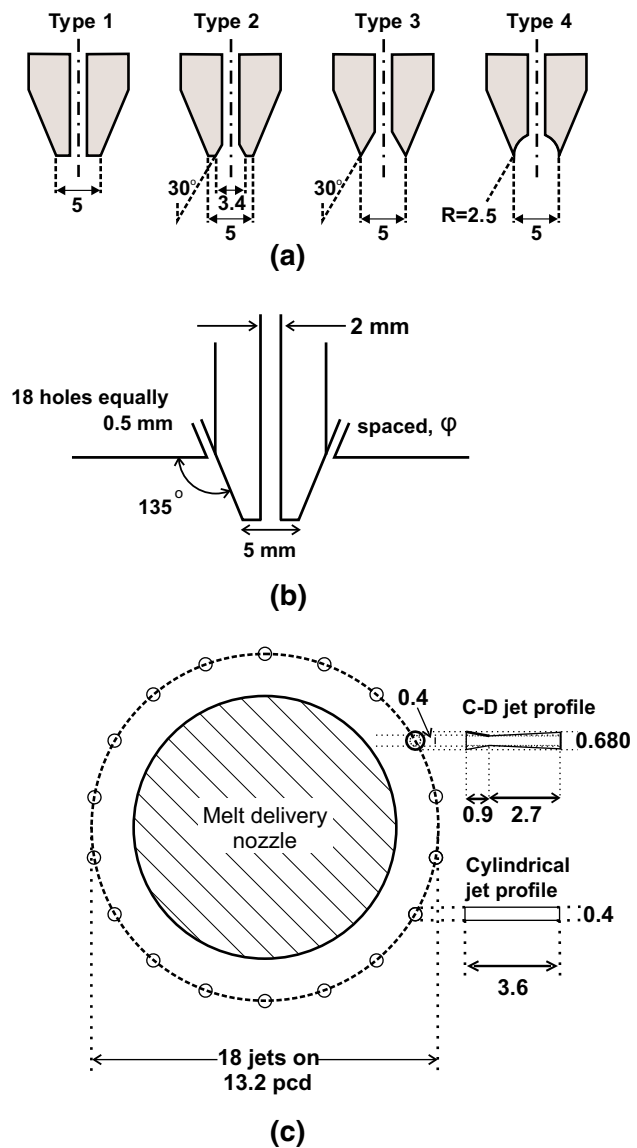


Fig. 3—Schematic view of (a) the four melt nozzle used in this study, (b) the annular slit die and nozzle configuration in the analog atomizer (shown for nozzle type 1), and (c) the choked and C–D gas jet profile and the discrete jet arrangement in the gas die.

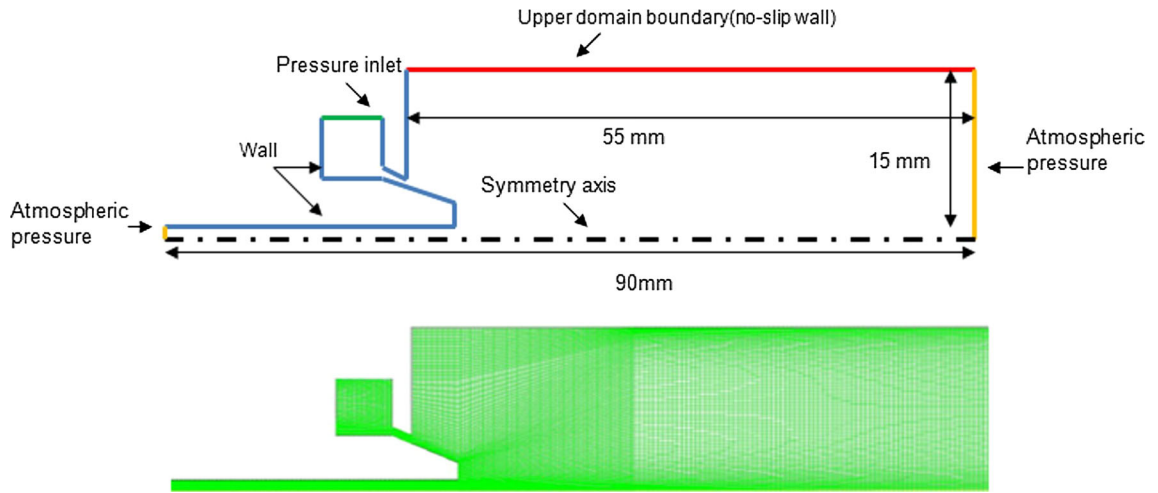


Fig. 4—The boundary conditions and mesh applied on the numerical domain.

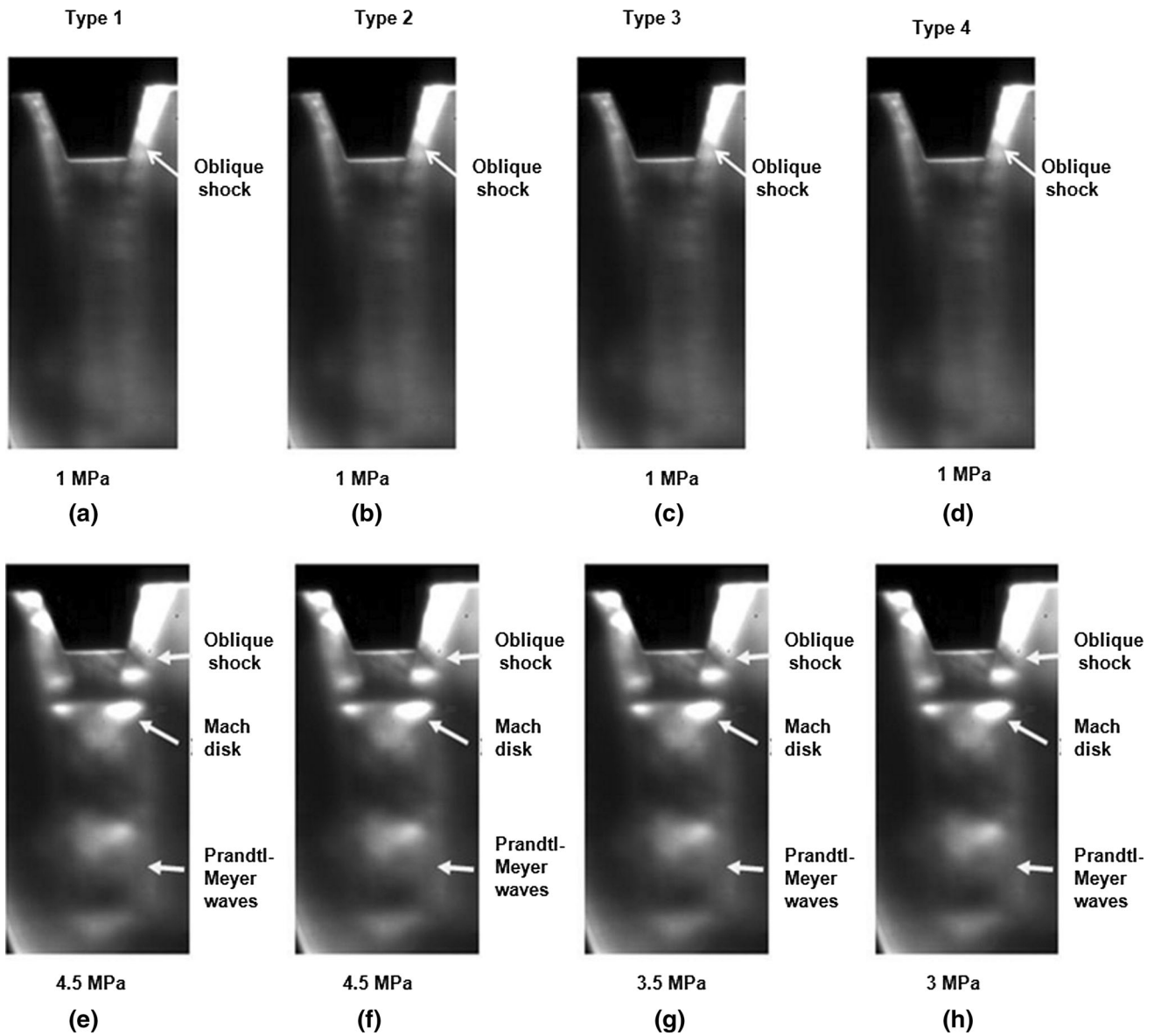


Fig. 5—Schlieren images of the gas flow around the four melt delivery nozzles investigated in this study when used with a choked (cylindrical) die. Upper row shows flow in the open-wake condition at a pressure of 1 MPa, and lower row shows flow in the closed-wake condition at the WCP.

diameter. This is achieved by rotating the EDM wire at an angle offset from that of the axis of the pilot hole. Four different melt nozzle designs (designated here types 1 to 4) were made from brass and mounted on the analog atomizer. Figure 3 shows the details of the various geometries considered for the melt delivery nozzles in this study, gives a schematic view of nozzle/die assembly, and shows the choked and C–D gas jet profiles.

III. NUMERICAL MODEL PROCEDURE

The commercial CFD code ANSYS Fluent 13 was used to solve the set of mass, energy, and momentum conservation (Reynolds Navier–Stokes) equations using a finite volume approach. Based on the Schlieren imaging study, in which very steady flow was observed, solutions were restricted to the steady-state case. A range of different two-equation turbulence models were applied during the investigation, with the results being relatively insensitive to the choice made, providing confidences in the numerical calculations presented. The SST $k-\omega$ model has been applied in the results presented here to close the Reynolds stress terms in the turbulence model. The CFD sensitivity to the turbulence

model used is considered in more detail by Motaman *et al.*^[11] The molten metal was omitted from the model as the aim of this study is to understand the simplified situation of the high-velocity gas jet flow behavior around the melt delivery nozzle. The SIMPLE algorithm was applied with an implicit second-order upwind scheme to solve the governing equations. The governing equations were solved for the $r-z$ components of a cylindrical system which is independent of ϕ , this having previously have been shown to be a reasonable approximation in this case by Ting *et al.*,^[7] Mi *et al.*,^[8] and Tong *et al.*^[9] The computation domain and the nozzle outlined are shown in Figure 4, with the flow direction being from left to right.

In order to evaluate the effect of meshing on the CFD results, a series of high-quality meshes were developed on the numerical domain with the increasing spatial resolution of 9000, 11000, and 18000 elements. It was established that the results, where the meshes contained 11000 elements or more, were acceptably mesh independent, and these were subsequently used for the simulations reported here. More details of mesh-independence study are discussed in Motaman *et al.*^[11]

A range of atomization gas pressures from 1 to 5.5 MPa were considered for the pressure inlet boundary condition to the gas inlet (in the case of the C–D die

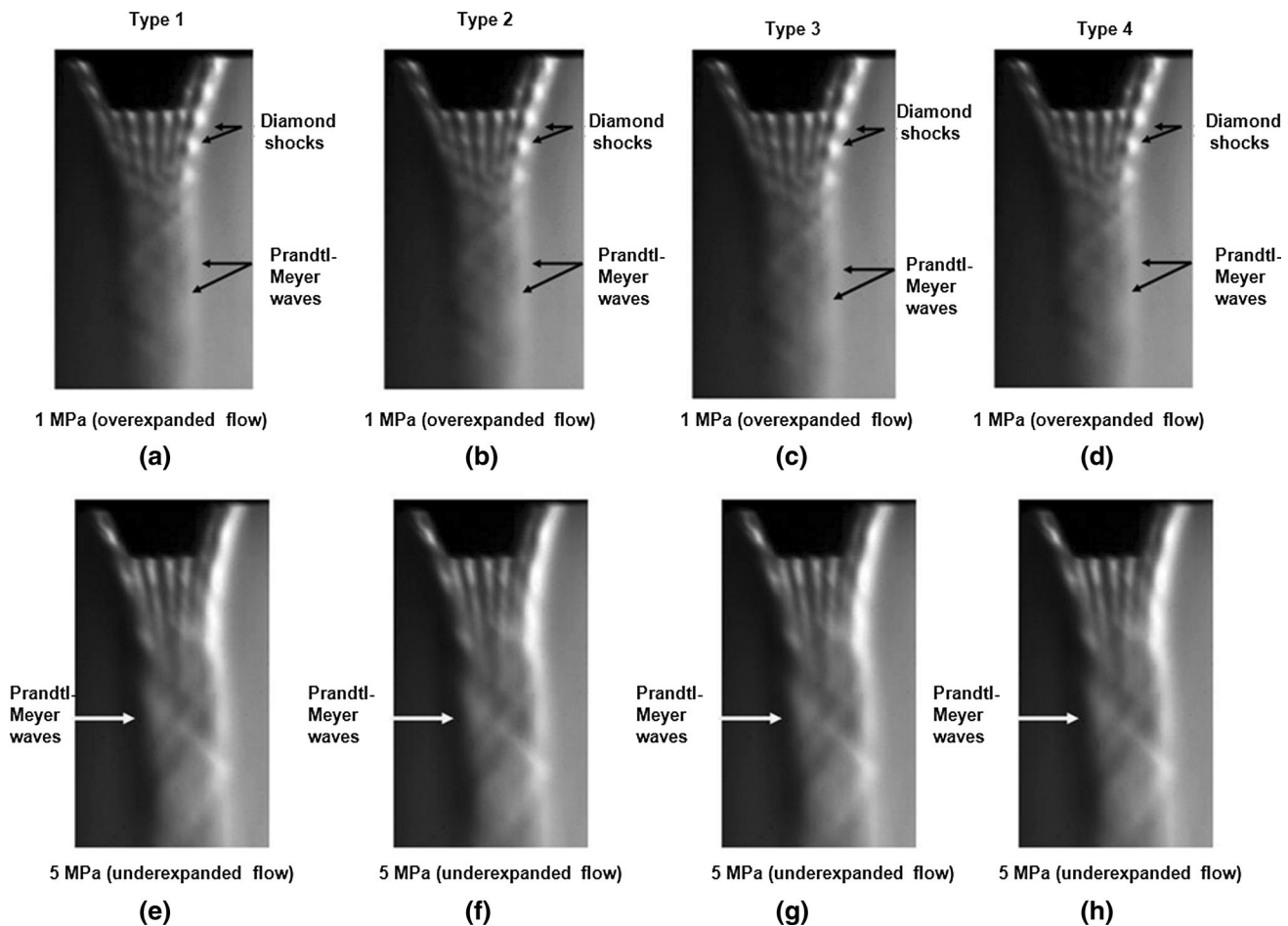


Fig. 6—Schlieren images of the gas flow around the four melt delivery nozzles investigated in this study when used with a C–D die. Upper row shows flow at a pressure of 1 MPa, and lower row shows flow at a pressure of 5 MPa. All cases are in the open-wake condition.

gas pressures below 2 MPa lead to an overexpanded flow, while pressures above 2 MPa lead to an underexpanded flow). The outlet of the domain (downstream of the melt nozzle) was taken as a pressure condition at atmospheric pressure. The outer boundaries of the chamber, melt delivery nozzle, and the gas die were considered as a wall with no-slip velocity condition. For the boundary labeled “Upper domain boundary” in Figure 4, two boundary models were considered, a wall with no-slip condition and an atmospheric pressure outlet. Calculations have been undertaken for both types of boundary condition. It was found that the results were comparable for both boundary conditions, and, as such, the wall boundary was used, since this provided consistently more convergence. In addition, for the thermal boundary conditions, at the upper boundary flows at inlet and outlet, the gas temperature was set at 300 K (27°C). In summary, the assumptions made in regard of the numerical model may be stated as follows:

1. Flow is considered to be steady state.
2. The effects of gravity are neglected.
3. Flow is 2D axis-symmetric.
4. Flow is considered as air and modeled as a compressible ideal gas.
5. The impact of the molten metal is not considered.

IV. RESULTS

A. Schlieren Imaging of Gas Flow with the Choked (Cylindrical) Die

Analog atomization experiments were undertaken for each of the four nozzle types, with both the choked (cylindrical) and C–D gas delivery dies, at pressures of 1 to 5 MPa, with the pressure being increased in 0.5-MPa increments. Figure 5 (upper figure) shows a still set of images of the gas flow around nozzle types 1 to 4 at gas pressure of 1 MPa with the choked gas die. At this inlet

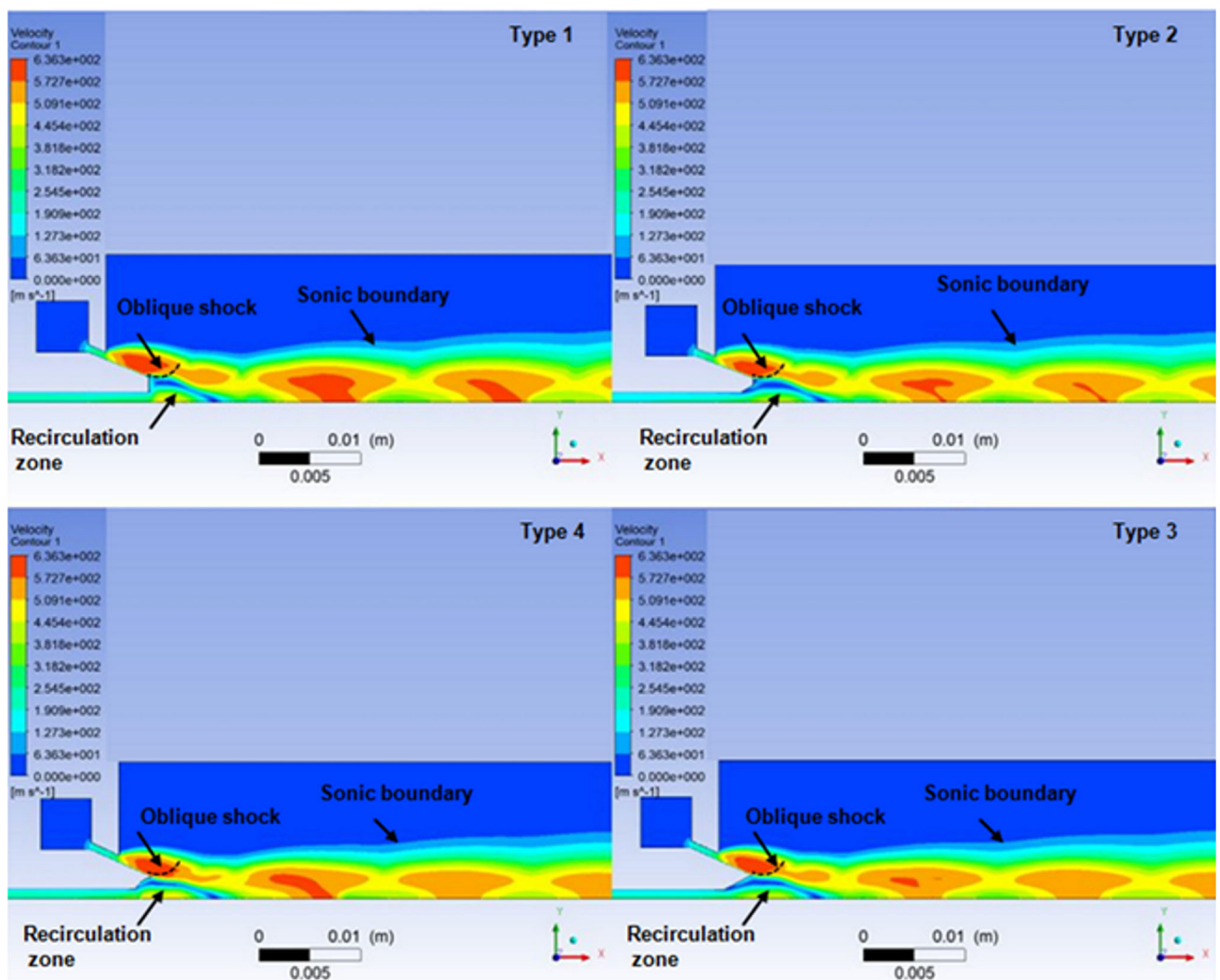


Fig. 7—CFD velocity contours (m s^{-1}) for the four melt delivery nozzles investigated in this study when used with a choked (cylindrical) die at a gas inlet pressure of 1 MPa.

pressure, upon exiting the die the gas is above ambient pressure, resulting in the generation of a series of oblique shocks around the melt nozzle tip. These shocks reduce the gas jet velocity. The gas then cyclically reaccelerates and decelerates to form a set of Prandtl–Meyer waves downstream from the melt nozzle tip. At this pressure, all nozzles are in open-wake condition.

With the increasing gas pressure, each of the nozzle types progressively undergoes a transition from the open- to closed-wake condition, although the pressure at which this occurs varies considerably with the internal profile. Nozzle type 4 undergoes this transition first, at a pressure of 3 MPa, followed by type 3 at 3.5 MPa, with the highest transition pressure (4.5 MPa) being observed for types 1 and 2 (Figure 5 lower part). The Mach disk is clearly evident in each of the images in the lower section of Figure 5, giving confidence in identifying the closed-wake condition in each case.

B. Schlieren Imaging of Gas Flow with the C–D Die

The gas-flow pattern for the four nozzles being investigated when used with the C–D gas die at gas pressures of 1 and 5 MPa are shown in Figure 6. At a pressure of 1 MPa (upper figure), an overexpanded flow is expected, with Prandtl–Meyer waves being observed about 3D downstream from the melt nozzle tip. Small diamond shocks around the circumferential edge of the melt nozzle tip are also evident. Broadly similar results are obtained for all pressures below 2 MPa.

On increasing the gas pressure to more than 2 MPa, a different flow pattern is observed. Figure 6 (lower part) shows the observed gas-flow pattern at an inlet pressure of 5 MPa; although, as above, the flow pattern is relatively insensitive to the actual pressure applied to the gas die in the range from 2 to 5 MPa. The emerging jets are now expected to be underexpanded and Prandtl–Meyer waves can be seen. Interestingly, at all pressures

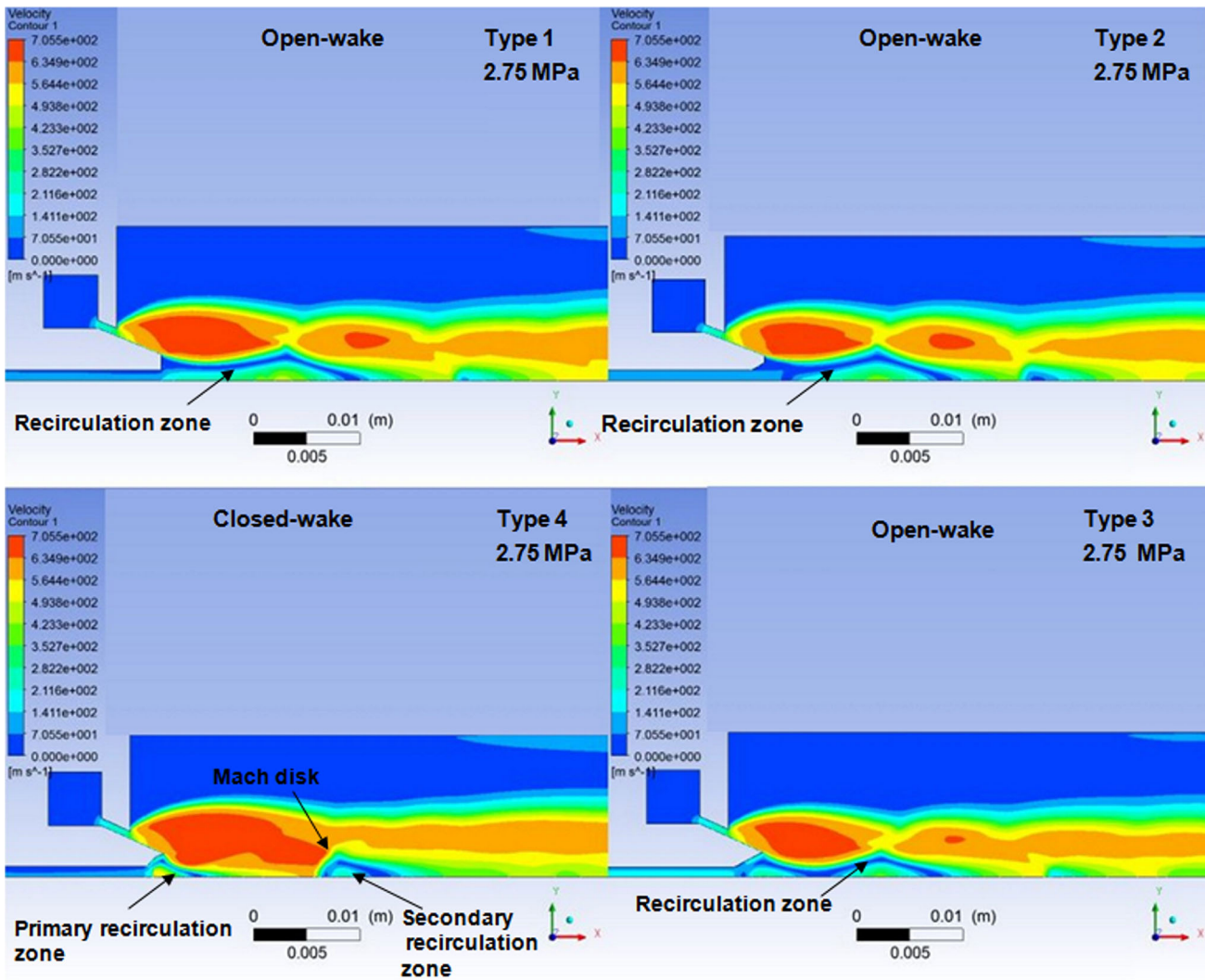


Fig. 8—CFD velocity contours (m s^{-1}) for the four melt delivery nozzles investigated in this study when used with a choked (cylindrical) die at a gas inlet pressure of 2.75 MPa.

up to 5 MPa, and irrespective of whether the gas flow is in the over- or underexpanded condition, the system remains in the open-wake condition for all nozzles. On the other hand, it is expected that the closed-wake condition should be observed at sufficiently high pressure, and we must conclude that the WCP is above 5 MPa for all nozzle types. However, pressures above 5 MPa were not available within the experimental system used.

Consequently, from the results presented above, we conclude that the transition from the open-to closed-wake condition occurs at significantly higher pressure when using a C–D die, relative to the otherwise identical configuration when using a choked (cylindrical jet) gas die.

C. CFD Simulation of Gas Flow with the Choked (Cylindrical) Gas Die

Velocity contours for the four different melt nozzles at an atomization gas pressure of 1 MPa, using the choked

gas die are given in Figure 7. For all nozzles, the high-velocity gas jet can be seen to expand rapidly immediately upon exiting the die. At this pressure, the flow is in the open-wake condition, which we determine from the absence of a Mach disk in front of melt nozzle. Due to the rapid expansion of the gas upon exiting the die, oblique shocks are formed around the melt nozzle tip, which slow down the gas flow in order to match the surrounding atmospheric pressure. The gas then undergoes a series of rapid, cyclic accelerations and decelerations producing a series of Prandtl–Meyer waves along the central axis of the simulation. The velocity field for all nozzles at this pressure is very similar.

Upon increasing the gas pressure to 2.75 MPa, the recirculation zone for type 1 has extended further downstream of melt nozzle tip, but the flow is still in the open-wake condition. A similar situation was also observed for nozzles 2 and 3 at this pressure (Figure 8). In the nozzle type 4, the expansion wave extends down to the central axis, forming a Mach disk, and consequently, a closed-wake condition was observed in this

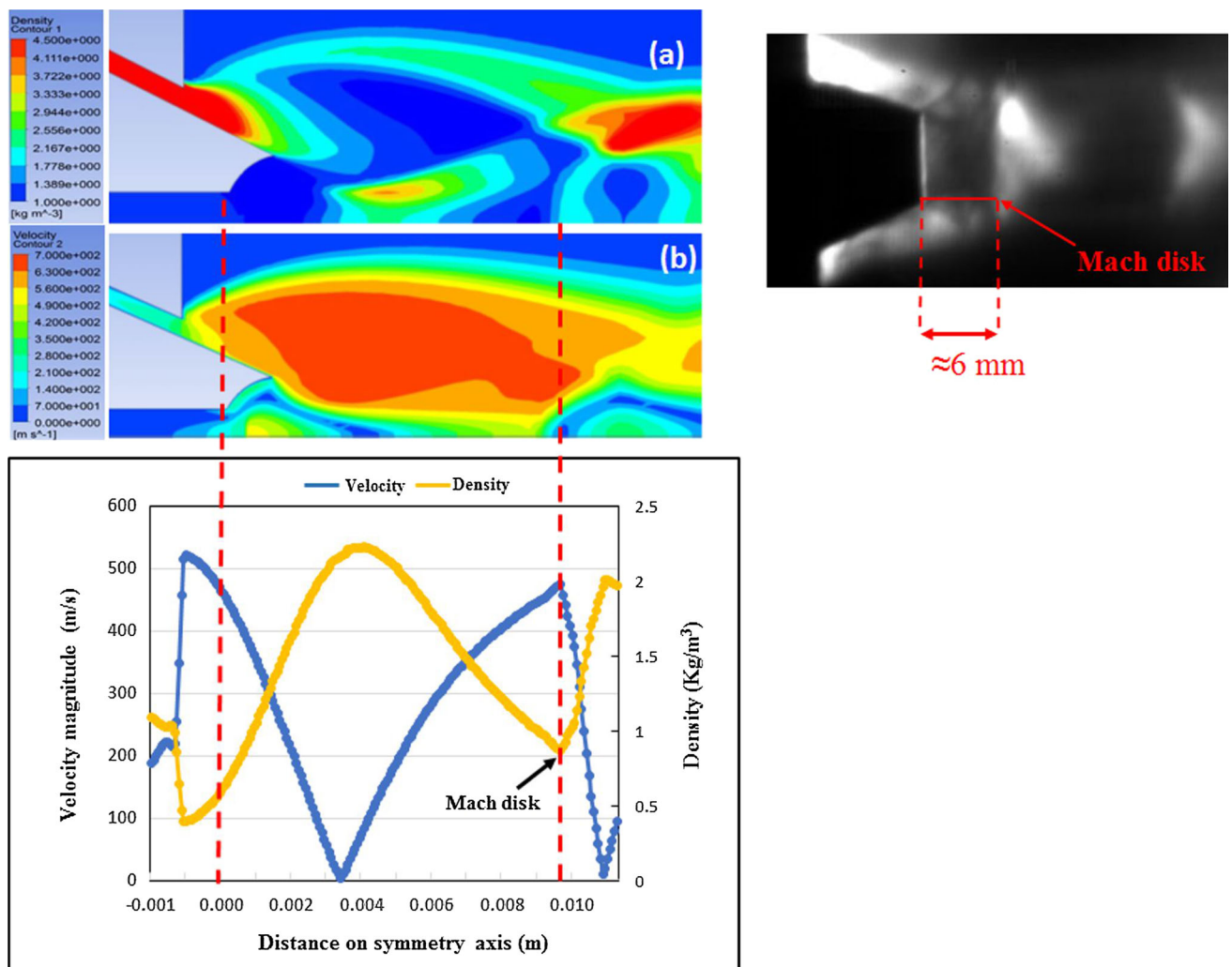


Fig. 9—Comparison of the CFD and experimentally determined positions of the Mach disk for nozzle type 4 with a choked gas die at an inlet pressure of 3 MPa.

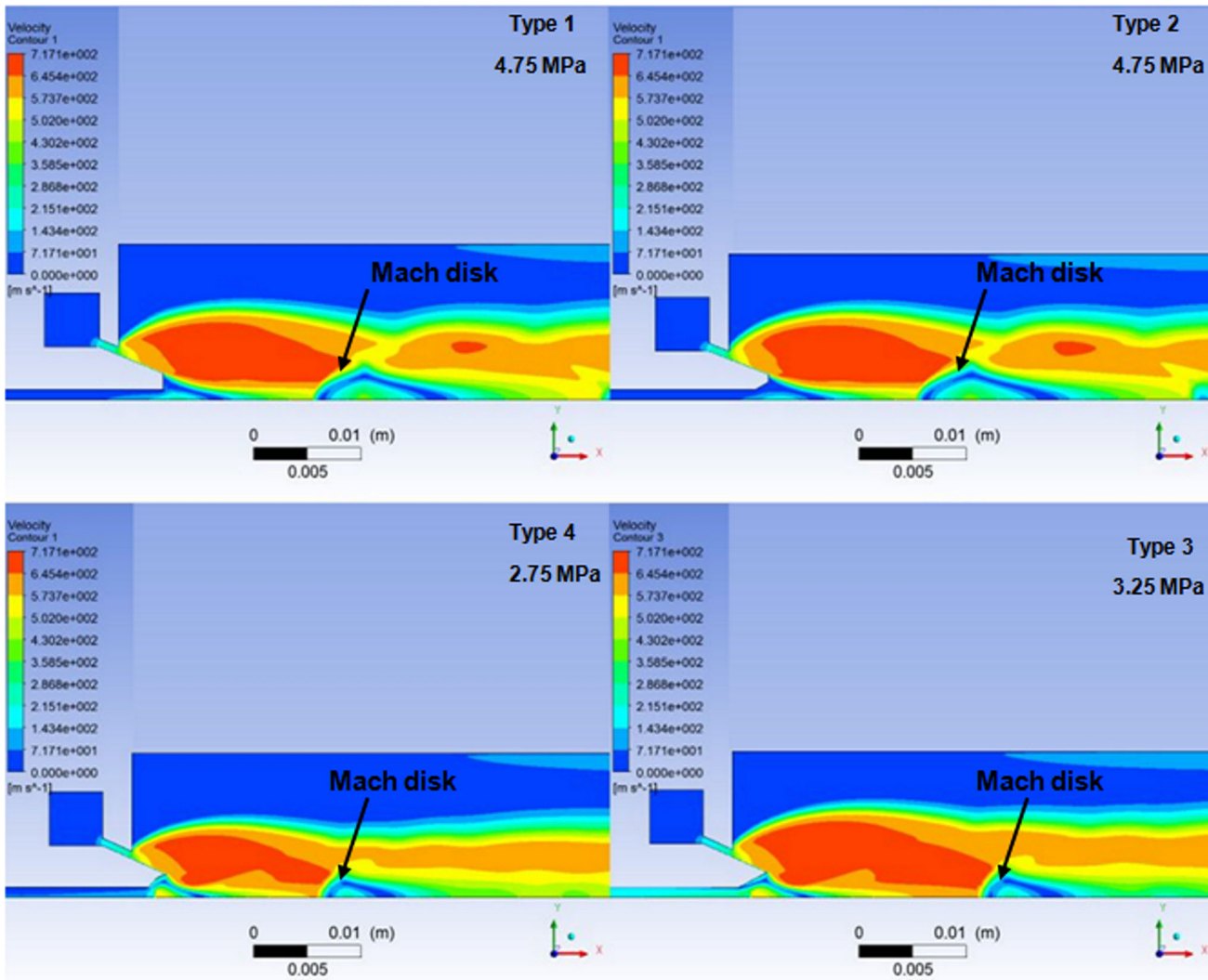


Fig. 10—CFD velocity contours (m s^{-1}) for the four melt delivery nozzles investigated in this study when used with a choked (cylindrical) die at WCP.

case. Due to the closed-wake condition, the recirculation zone for nozzle type 4 was truncated, and two recirculation zones have emerged: one downstream of the melt nozzle tip and the other downstream of the Mach disk (Figure 8). By way of a quantitative validation of the numerical results, the positions of Mach disk for nozzle type 4 at an inlet pressure of 3 MPa is shown for both the Schlieren image and CFD simulation in Figure 9, wherein a good agreement may be observed.

At an atomization gas pressure of 3.25 MPa, the gas flow in nozzle types 1 and 2 was still in the open-wake condition. However, in nozzle type 3, a Mach disk was formed, and the gas flow had transformed from the open- to closed-wake condition. For nozzles types 1 and 2, this transition is observed at 4.75 MPa. Figure 10 shows the closed-wake condition for these nozzles at WCP. In all cases, the gas-flow pattern in the closed-wake condition shows two recirculation zones: one

between the melt nozzle tip and the Mach disk and other downstream of Mach disk.

D. CFD Simulation of Gas Flow with the C–D Gas Die

A velocity contour plot for the four types of melt nozzles being investigated when combined with the C–D gas die are depicted in Figure 11 for a gas inlet pressure of 1 MPa. At this pressure, the gas flow is overexpanded. The gas flow downstream of the melt nozzle is in the open-wake condition, with a series of Prandtl–Meyer waves being formed further downstream. Similar results are observed at all pressures up to 5 MPa (images are not presented), irrespective of whether the gas emerging from the jets is in the over- or underexpanded condition. This is consistent with the experimental data, wherein no significant change in the wake condition was observed with increasing gas pressure. However, by increasing the

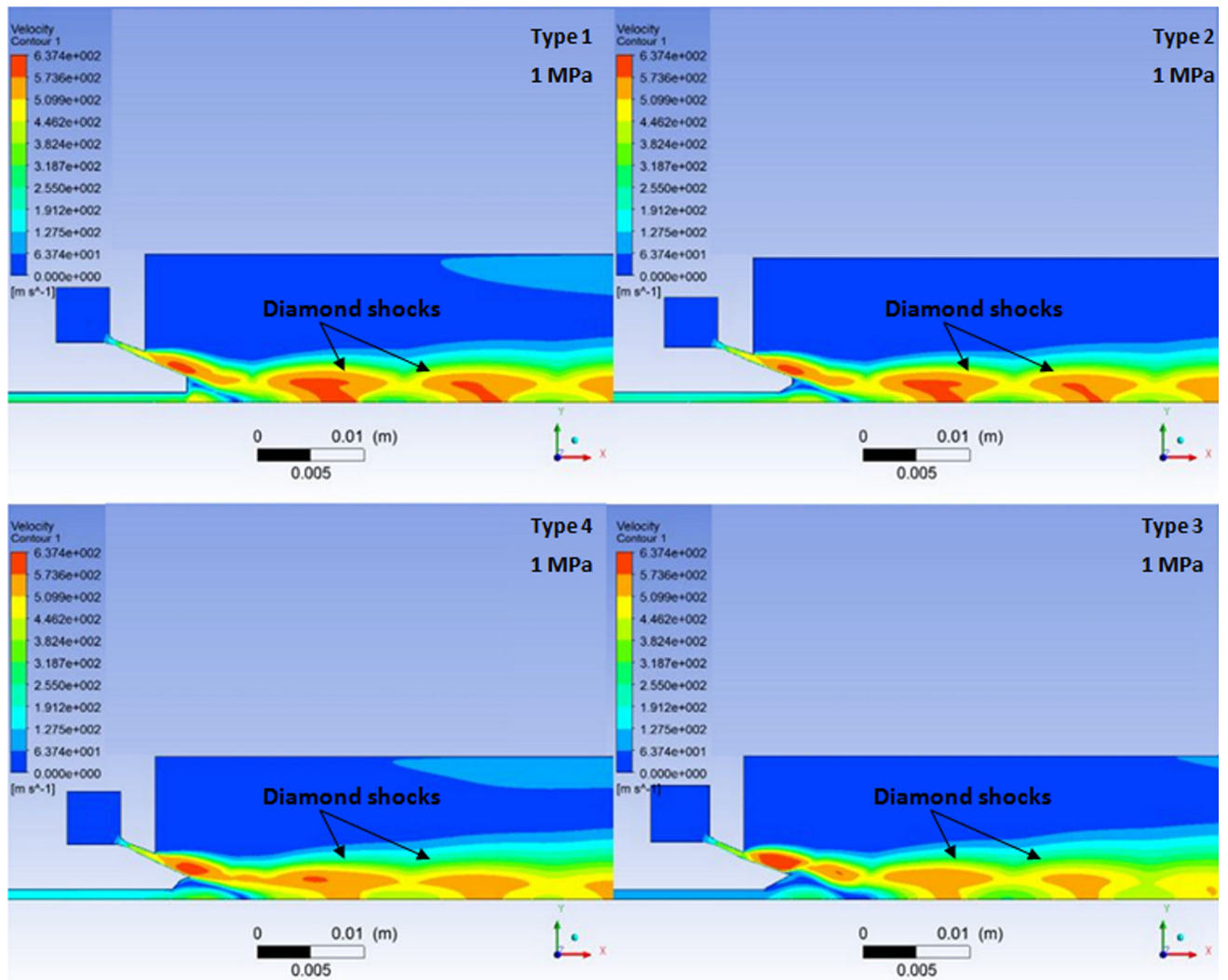


Fig. 11—CFD velocity contours (m s^{-1}) for the four melt delivery nozzles investigated in this study when used with a C–D die at a gas inlet pressure of 1 MPa (overexpanded flow).

Table I. The WCP for Different Melt Nozzles with Two-Gases Die System

Gas Die Type	Melt Nozzle Type			
	Type 1	Type 2	Type 3	Type 4
Cylindrical die at experimental (MPa)	4.5	4.5	3.5	3
Cylindrical die at CFD (MPa)	4.75	4.75	3.25	2.75
C–D die at CFD (MPa)	5.3	5.3	5.15	5.1

gas pressure above 5 MPa, wake closure was observed in all four nozzles, with the estimated values for the WCP being shown in Table I.

Figure 12 shows the closed-wake condition for all nozzles at WCP for each of melt nozzle in Table I. In nozzles types 1 and 2, the closed-wake condition, as evidenced by the formation of a Mach disk, occurred at 5.30 MPa, while in nozzle types 3 and 4, it occurred at pressures of 5.15 and 5.1 MPa, respectively. It seems that, as with the choked die, the closed-wake condition

occurs in nozzle types 1 and 2 at a higher gas pressure than for nozzle types 3 and 4, although the difference in WCP between the four nozzles is much reduced compared with the case in which a choked die is used.

V. DISCUSSION

The experimental and CFD studies show that the most significant difference in WCP was observed between nozzle

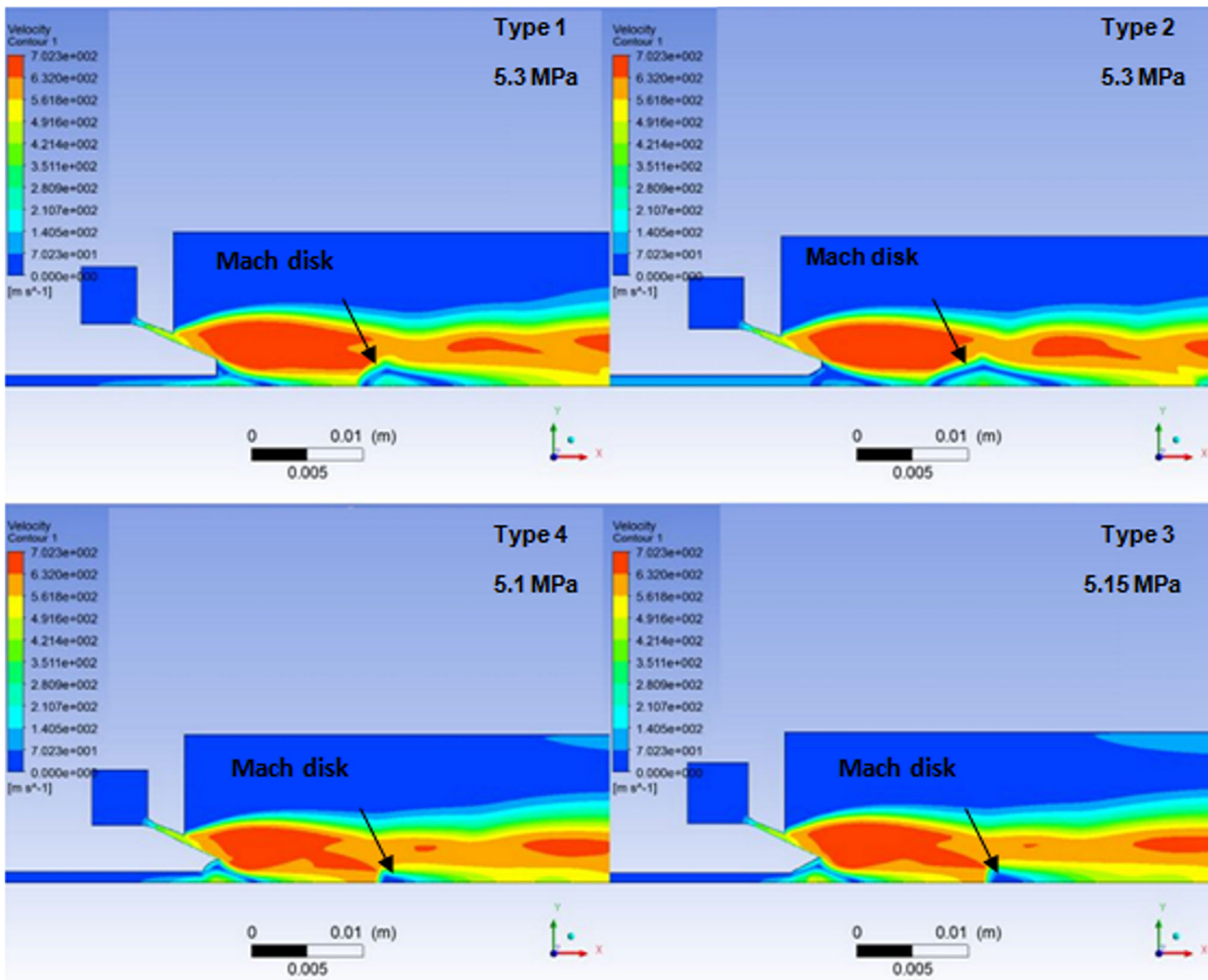


Fig. 12—CFD velocity contours (m s^{-1}) for the four melt delivery nozzles investigated in this study when used with a C–D die at WCP.

types 1 and 4. The transition between the open- and closed-wake conditions appears to be influenced by the combined effects of the internal profile of the melt nozzle and the shape of the resulting recirculation zone that forms. A useful first step is to clarify how the closed-wake occurs for each nozzle at WCP in terms of considering how the flow behavior changes as inlet pressure increases. To aid with this explanation, nozzle type 1 has been chosen as a reference case to investigate the flow behavior leading to WCP. The behavior of the other nozzles can then be understood relative to this case. In the experimental and CFD study, this nozzle was observed to have a WCP of 4.5 and 4.75 MPa, respectively, for the choked die. The key flow behavior observed as the pressure is increased toward WCP for nozzle type 1 is outlined in Figure 13.

As seen in Figure 13, at a gas pressure of 1 MPa the open-wake condition is evident; the gas leaves the die and is seen to expand rapidly as it moves away from the die exit. It forms a “convex lens” shape as the flow first expands and then contracts. This situation causes recompression shocks to form around the circumferential

edge of the melt nozzle tip, which reduce the gas velocity. The gas reaccelerates and then decelerates forming a set of Prandtl–Meyer waves along the central axis. It can be seen that a recirculation zone forms just downstream of the melt nozzle tip and beneath the expanding gas jet. Increasing the gas pressure to 2 MPa causes an expansion of the convex lens shape gas wave in both directions (length and width). The recirculation zone, which is surrounded by the expanding gas wave, is squeezed downward by the expanding gas wave. This causes a change in both shape and size of the recirculation zone compared with the previous lower inlet gas pressure (Figure 13). Finally, at the WCP (4.75 MPa), the recirculation zone is pinched off by the further expansion of the gas wave, and a Mach disk is seen to form. The transition to the closed-wake condition is due to the expanding gas increasing in size to the extent that it reconnects with itself on the central axis. It is important to note that this mechanism for the transition from the open- to closed-wake condition is observed to occur in a similar manner (expanding gas wave reconnecting

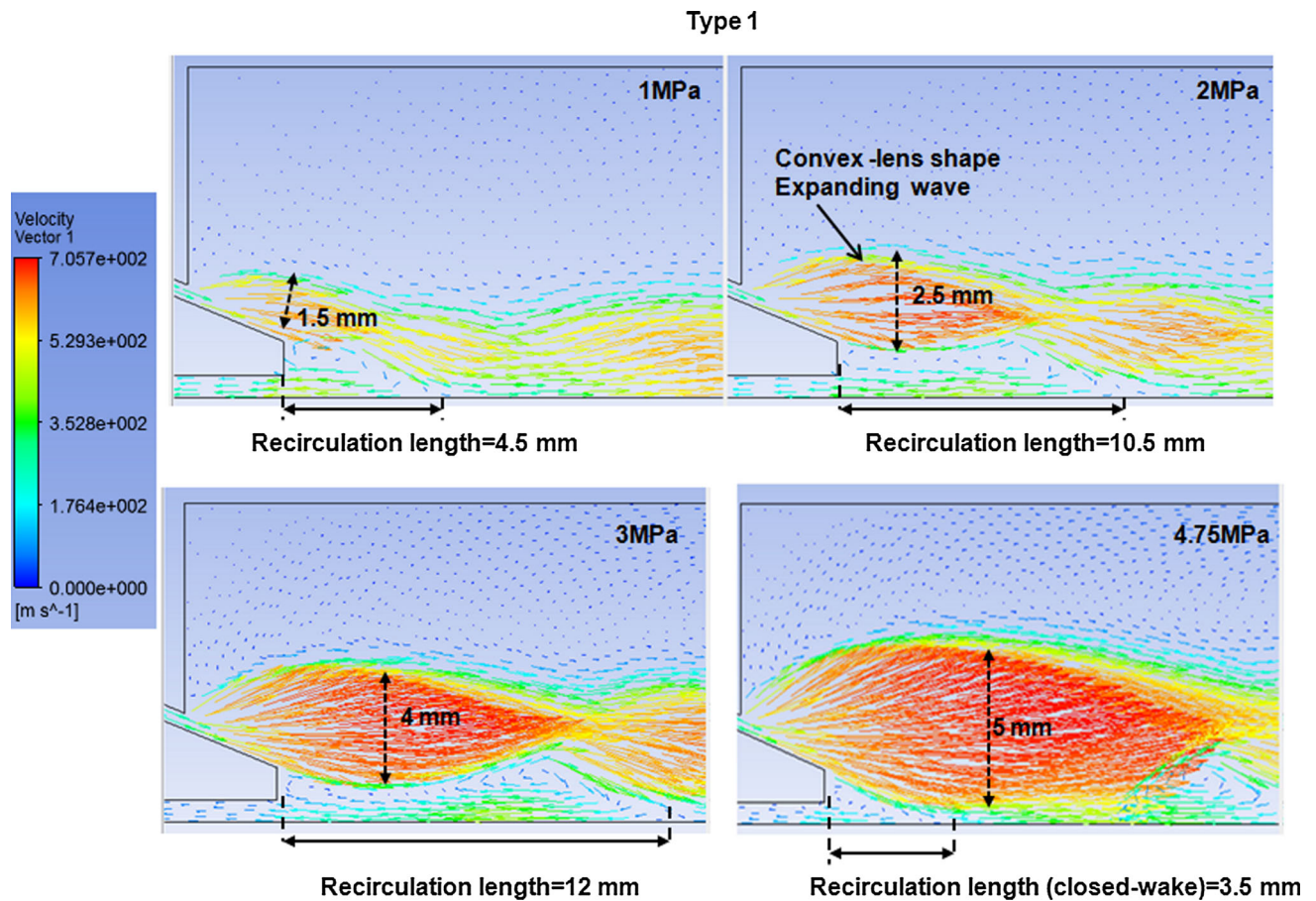


Fig. 13—The velocity vector field, as a function of gas inlet pressure, around a type 1 nozzle when using a choked die.

with itself on the central axis) for all nozzle types tested in the experiments, but at different gas pressures.

The open- to closed-wake transition for nozzle type 1 with the C–D gas die also was seen to follow the same trend, but with the C–D gas die always transitioning at a higher WCP. Moreover, the difference between the WCP for the various nozzles considered was much smaller when the C–D die was utilized, relative to that for the choked die. To investigate this behavior, the difference in the gas flows between the choked and C–D gas die (for a given nozzle design) is considered. Figure 14 shows the velocity fields for a type 1 nozzle with both a C–D and a choked gas dies at the same gas inlet pressures. As noted, a higher WCP is found in the case of the C–D design. The reason for this can be understood in the context of how the wake closure occurs. In the case of the C–D design, upon exiting the die, the jet does not expand to the same extent as the choked design, with a more collimated jet for the C–D gas die compared with choked die (Figure 14). This is to be expected, since for the choked die, the inlet and outlet gas pressures will be the same, whereas for the C–D die the outlet pressure is approximately 1/20 of the inlet pressure due to the controlled expansion of the gas inside the jet. For both dies, when considered individually, the width of the expanding gas wave increases

in an approximately linear manner with jet exit pressure. However, no correlation of expansion wave width with pressure is possible between dies as the exit pressure is very much lower in the C–D die than in the choked die.

In the case of the choked design, the larger width of the expanding wave pinches off the recirculation zone at a lower gas pressure compared with the C–D gas die (Figure 14), and hence the lower WCP. It should be noted that a similar trend is observed for all melt nozzles, regardless of the melt tip geometry, with WCP occurring at a higher pressure for the C–D case. This condition is also supported by the argument of Ting *et al.*^[3] that the WCP for a C–D gas die was measured at a gas pressure of about 5 MPa.

The next step is to consider why WCP depends upon melt nozzle tip design. For this purpose, nozzle type 4 is compared with type 1, as these two types show the most significant difference in WCP. Figure 15 compares the velocity vector fields for the choked and C–D dies in these two nozzles. The lengths of the convex-lens shaped, expanding gas waves for both nozzles designs are not significantly impacted by the change in pressure—being 4.5 mm at 1 MPa and 9 mm at 2 MPa, irrespective of nozzle design. However, the shapes of the expansion wave are different. As the gas pressure is increased from 1 to 2 MPa, each nozzle displays a

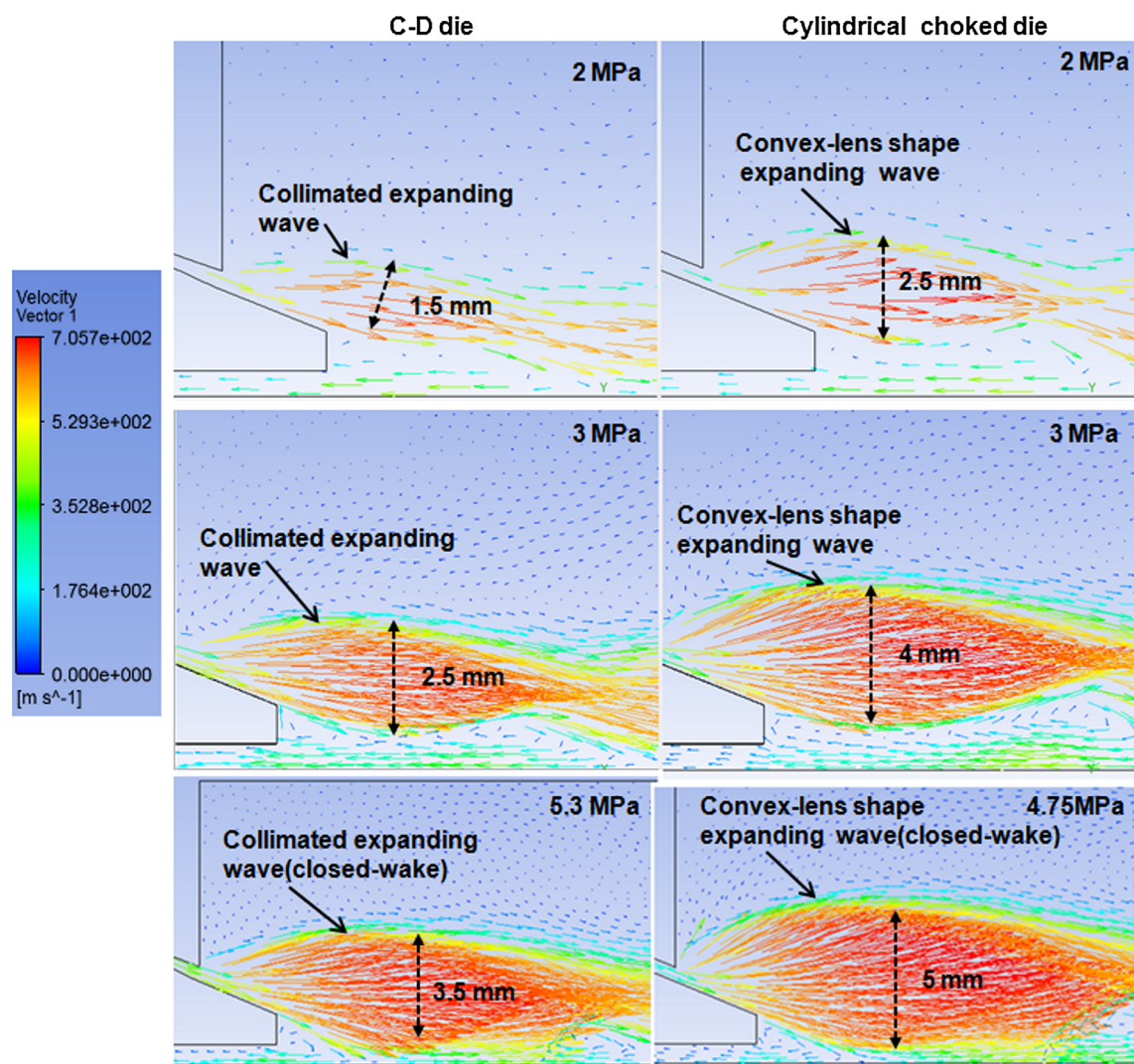


Fig. 14—Comparison of the velocity vector fields, as a function of gas inlet pressure, around a type 1 nozzle, when used with choked and C–D dies.

convex-lens shaped gas wave that expands in both length and width, but in the type 1 nozzle this is restricted in width.

As also shown in Figure 15, the lengths and shapes of the recirculation zone formed in front of the melt tip are different for the two nozzles. The hemispherical shape of type 4 results in a recirculation zone that produces a flow of gas inside the melt tip cavity. As a result, this changes the direction at which the gas in the recirculation zone meets the incoming gas from the die (Figure 16). Whether these are causally related or manifestations of the same underlying cause is difficult to establish. The direction in which the recirculating gas meets the incoming gas will alter the momentum balance in this system. Equally, the shape of the melt delivery nozzle influences the formation and direction of oblique shocks at the nozzle tip, which could affect both the recirculation pattern and the downstream gas expansion wave. In this respect, we note that the introduction of

convex/concave surface is common practice in the aerospace industry to alter the direction and the significance of oblique shocks.

VI. CONCLUSIONS

Use of a combination of CFD and Schlieren imaging techniques for observing and simulating the gas-flow patterns around the melt delivery nozzle of a Close-Coupled Gas Atomizer (CCGA) has revealed reasonable agreement between the numerical and experimental results in determining the WCP. Observation of gas-flow patterns around four different types of melt nozzles and with two gas die systems (choked and C–D) revealed a strong, and perhaps unexpected, effect on WCP which is very sensitive to the even a small change in the melt tip geometry. According to the CFD and the experimental results, the closed-wake condition is achieved with a

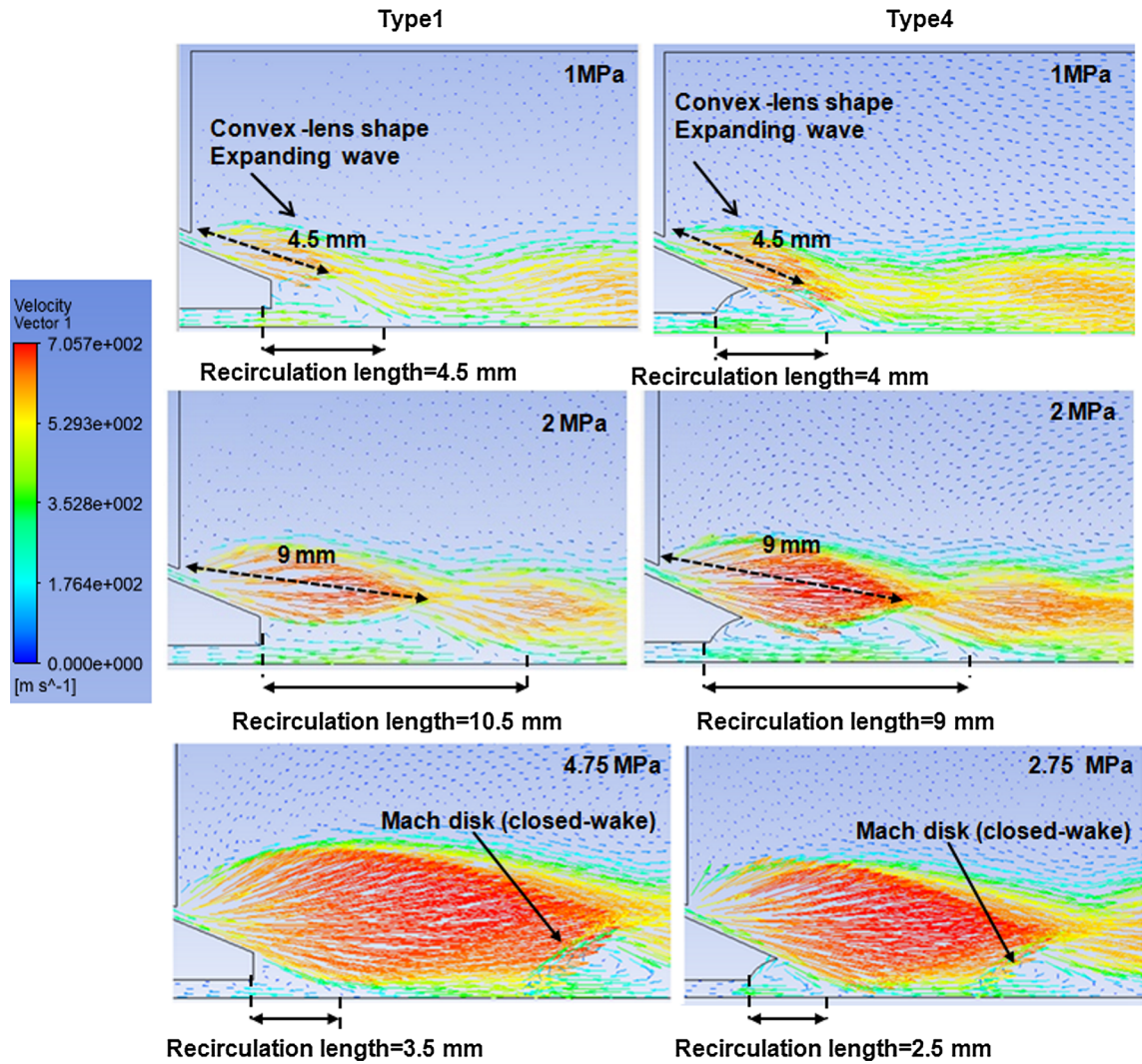


Fig. 15—Comparison of the velocity vector fields, as a function of gas inlet pressure, around a type 1 and a type 4 nozzle, when used with a choked die.

choked die at atomization gas pressures of 4.5 MPa for nozzle types 1 and 2, 3.5 MPa for type 3, and 3 MPa for type 4. On the other hand, the C–D gas die tested in this investigation, which was designed to produce ideal expansion at an inlet gas pressure of 2 MPa, did not display wake closure with any nozzle until the gas pressure exceeded 5 MPa, and only a very weak dependence of WCP upon nozzle geometry was observed. However, it should be stressed that these results apply to the specific C–D gas die design in this test, and the WCP may be different if, for instance, the apex angle or internal profile of the C–D gas die was changed. Although Ting *et al.*^[3] reported that atomizer operation at such high gas pressures and close to the WCP condition may produce finer particles, it will also increase production costs and gas consumption. Finding the appropriate matching designs of die and nozzle, and optimizing the operating conditions for the pairing, remains a significant challenge for atomizer designers.

This research also proposed a new explanation regarding open- and closed-wake conditions for different melt tip designs. Building upon the previous model by Ting *et al.*,^[3] which laid much of the fundamental understanding of the wake closure phenomenon, the model proposed in this research explains the open- to closed-wake transition as a function of gas die and melt tip design in more detail. It was found that the closed-wake condition occurs when the convex-lens shapes expanding gas wave expands gradually with the increasing inlet gas pressure until it pinches off the recirculation zone. Comparison between the velocity fields produced by the choked and C–D gas dies at the same inlet gas pressure showed that the convex-lens shaped gas wave in the C–D die is more collimated than that in the choked gas die, leading to a higher WCP for the C–D die. Comparing the velocity fields between different nozzle types showed that the melt tip profile design affects the shape and length of the recirculation zone. As a result,

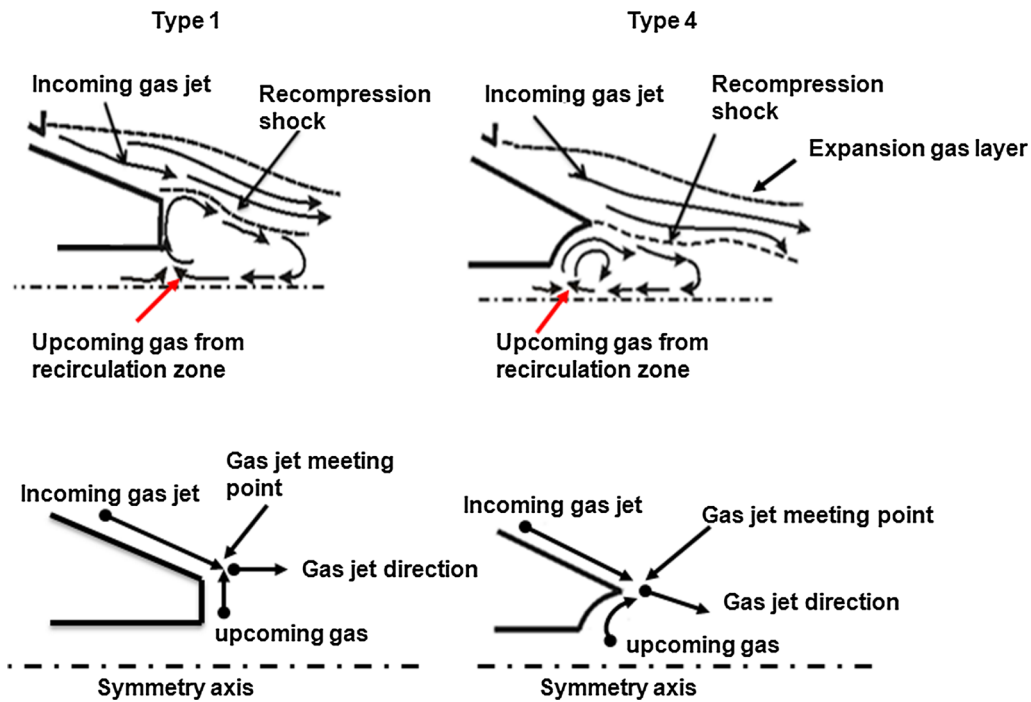


Fig. 16—The schematic view of gas flow and gas jet's meeting point for nozzles types 1 and 4 at open-wake condition and at atomization gas pressure of 1 MPa.

nozzles with an internal cavity (types 3 or 4 as studied here) help the convex-shaped expanding wave expand further downward to the recirculation zone and pinch off this region at a lower gas pressure (lower WCP).

REFERENCES

1. I.E. Anderson, R.S. Figliola, and H. Morton: *Mater. Sci. Eng.*, 1991, vol. 148, pp. 104–14.
2. I.E. Anderson, R.L. Terpstra, and R.S. Figliola: *Adv. Powder Metall. Part. Mater.*, 2004, vol. 2, pp. 26–36.
3. J. Ting, M.W. Peretti, and W.B. Eisen: *Mater. Sci. Eng.*, 2002, vol. 326, pp. 110–21.
4. S.P. Mates and G.S. Settles: *Adv. Powder Metall. Part. Mater.*, 1995, vol. 2, pp. 1–15.
5. S.P. Mates and G.S. Settles: *Atom. Spray*, 2005, vol. 15, pp. 20–27.
6. I.E. Anderson and R.S. Figliola: *Mod. Dev. Powder Metall.*, 1998, vol. 20, pp. 205–23.
7. J. Ting and I.E. Anderson: *Mater. Sci. Eng. A*, 2004, vol. 379, pp. 264–76.
8. J. Mi, R.S. Figliola, and I.E. Anderson: *Metall. Mater. Trans. B.*, 1997, vol. 28B, pp. 935–41.
9. M. Tong and D.J. Browne: *Comput. Fluids*, 2009, vol. 38, pp. 1183–90.
10. Z. Xinming, J. Xu, Z. Xuexin, and Z. Shaoming: *Sci. China Ser. E*, 2009, vol. 52, pp. 3046–53.
11. S. Motaman, A.M. Mullis, R.F. Cochrane, I.M. McCarthy, and D.J. Borman: *Computers & Fluids*, 2013, vol. 88, pp. 1–10.